Available online at www.sciencedirect.com
SCIENCE DIRECT
Journal of Catalysis 239 (2006) 23–33
JOURNAL OF CATALYSIS
www.elsevier.com/locate/jcat

Influence of O_2 and H_2 on NO reduction by NH_3 over Ag/Al_2O_3: A transient isotopic approach

Evgenii V. Kondratenko *, Vita A. Kondratenko, Manfred Richter, Rolf Fricke

Leibniz-Institut für Katalyse e. V. an der Universität Rostock, Aussenstelle Berlin [1], Richard-Willstätter-Str. 12, D-12489, Berlin, Germany

Received 20 October 2005; revised 23 December 2005; accepted 7 January 2006

Available online 15 February 2006

Abstract

Mechanistic aspects of low-temperature (423–723 K) selective catalytic reduction of NO with NH_3 (NH_3-SCR) over an Ag(1.7 wt%)/Al_2O_3 ($2Ag/Al_2O_3$) catalyst in the presence and absence of O_2 and H_2 were studied using a transient low-pressure (peak pressure < 10 Pa) technique, the temporal analysis of products (TAP) reactor, in combination with isotopic traces. Preoxidized $2Ag/Al_2O_3$ showed very low activity in the NH_3-SCR reaction. The activity increased tremendously after ex situ reduction of $2Ag/Al_2O_3$ in a hydrogen flow (5 vol% H_2 in Ar) at 373 K for 30 min. This observation was related to the creation of reduced Ag species, which catalyze O_2 and NO dissociation, yielding adsorbed oxygen species. O_2 is a better supplier of oxygen species. Oxygen species played a key role in NH_3 dehydrogenation, yielding reactive NH_x fragments that are important intermediates for nitrogen formation via a coupling reaction between NO and NH_3. This reaction pathway predominated over direct NO decomposition to N_2 in the presence of O_2. In addition to generation of active oxygen species, gas-phase oxygen accelerated transformation of surface N-containing intermediates into gas-phase reaction products. The role of hydrogen in the NH_3-SCR reaction is to transform oxidized Ag species into reduced species that are active sites for O_2 and NO adsorption. Our findings suggest that the reduction of oxidized Ag is responsible for the boosting effect of H_2 in the NH_3-SCR reaction, and also that H_2 helps decrease total N_2O production.

Keywords: NH_3-SCR; Ammonia; Reaction mechanism; TAP reactor; Silver; Nitric oxide

1. Introduction

Selective catalytic reduction of NO_x with hydrocarbons (HC-SCR) in the presence of oxygen has potential applications in removing NO_x from automotive engines under lean conditions [1,2]. Alternatively, NH_3-assisted selective reduction (NH_3-SCR) of NO_x may become the basis of a future urea SCR technology for NO_x abatement from mobile diesel engines [3–6]. Since the pioneering work of Held et al. [7], many catalyst formulations have been prepared and tested for SCR reactions in the presence of O_2. Among the numerous catalytic materials applied, silver-containing catalysts exhibit high activity in the HC-SCR reaction at high temperatures [1,2]; however, they suffer from low activity at temperatures below 623 K. Recently, it was shown with the finding that the operating reaction temperature is shifted down to 473 K if hydrogen is fed to a lean exhaust gas mixture ($\lambda > 1$) [8,9]. Recently, Richter et al. [10] found a similar effect of H_2 on the low-temperature NH_3-assisted SCR of NO_x over the same type of Ag/Al_2O_3 catalysts. The NO conversion to N_2 increased from 10 to 100% at 473 K on cofeeding of H_2 to the feed mixture (1000 ppm NO, 1000 ppm NH_3, 6 vol% O_2, and 7 vol% H_2O in He).

Although the origin and the mechanism of this so-called "H_2 effect" for the HC-SCR reaction have been thoroughly investigated by many research groups, they remain incompletely understood. There seems to be agreement in the scientific community that a functionalized alumina (or zeolite) surface is indispensable, because neither Ag supported on α-Al_2O_3 nor Ag supported on silica shows any beneficial influence of H_2 on activity. The existence of well-defined Ag clusters is a suggested prerequisite for the H_2 effect [9–12].

Many authors have emphasized the role of hydrogen in formation or decomposition of certain adsorbed species. Burch et al. [13] suggested that H_2 helps prevent accumulation of

* Corresponding author.
E-mail address: evgenii@aca-berlin.de (E.V. Kondratenko).
[1] Former Institute for Applied Chemistry Berlin-Adlershof.

0021-9517/$ – see front matter
doi:10.1016/j.jcat.2006.01.008

Ag–CN species, which have very low activity in the HC-SCR reaction. Instead of Ag–CN species, organic cyanide species are formed in the presence of H_2. These species are expected to accelerate NO removal. But this effect is not observed at temperatures below 523 K. Satokawa et al. [9] ascribed the promoting effect of H_2 on the SCR reaction of NO with C_3H_8 to the promotion of hydrocarbon activation. This was concluded after taking into account the appearance of surface acetate and NCO species during the SCR reaction in the presence of H_2 only. Many authors have emphasized the role of nitrite/nitrate species in the SCR reactions [1,14–17]. Besides the heterogeneous nature of the H_2 effect, radical gas-phase reactions have been postulated to play a crucial role in the HC-SCR reaction in the presence of H_2 [18–20]. A proposed mechanism for the HC-SCR of NO_x in [19] includes gas-phase reactions of NO_x with N-containing organic intermediates. H_2 catalyzes the formation of these intermediates and activates NO_x species.

It should be emphasized that the above mechanistic concepts were developed based mainly on catalyst characterization studies using various physicochemical techniques. Despite the potential of transient techniques to provide considerably more mechanistic insight into individual steps of catalytic reactions compared with steady-state experiments, they have been applied in only a few cases for mechanistic analysis of the SCR reactions without drawing attention to the H_2 boosting effect [21–25]. Recently, the TAP reactor in combination with isotopic traces was shown to be an excellent tool for mechanistic investigations of high-temperature (above 973 K) ammonia oxidation and related processes over Pt and Pt–Rh gauze catalysts [26,27]. To the best of our knowledge, the TAP approach has not yet been applied for mechanistic analysis of the effect of H_2 on the selective catalytic reduction of NO with NH_3 over Ag/Al_2O_3 catalysts.

Consequently, the present study focuses on further elucidation of the effect of added hydrogen on the NH_3-SCR reaction over an Ag/Al_2O_3 catalyst. To complete the mechanistic picture, not only NO–NH_3–O_2–H_2, interactions, but also NO–NH_3 and NO–NH_3–O_2 interactions, were studied over preoxidized and prereduced Ag/Al_2O_3 catalysts using the TAP reactor at a temperature range of 423–723 K. This temperature range was chosen to cover the region where the accelerating effect of hydrogen was found for steady-state ambient pressure NH_3-SCR of NO over the same catalyst.

2. Experimental

2.1. Catalyst preparation

Details on the preparation procedure of Ag/Al_2O_3 catalysts have been described previously [10]. In brief, alumina hydrate powder (Disperal P2, CONDEA) was dispersed in water under intense stirring at room temperature for at least 30 min. Then an appropriate amount of 1 M $AgNO_3$ solution was added to the sol to achieve the desired Ag content. The gel thus formed was filtered and dried at 393 K for 2 h. The obtained powder was compacted to pellets and subsequently crushed yielding samples with mesh sizes (ASTM) of 42–24 (350–710 μm). In the present study, a sample with Ag loading of 1.73 wt% (designated as $2Ag/Al_2O_3$) was used. The silver content was determined by elemental analysis (OES-ICP). The alumina support (pretreatment at 873 K in air for 2 h) had a γ-Al_2O_3 phase structure after calcination, with a BET surface area of 235 $m^2\,g^{-1}$, a pore volume of 0.43 $cm^3\,g^{-1}$, and an average pore diameter of 5.2 nm. This texture was not significantly different for the $2Ag/Al_2O_3$ sample.

2.2. Transient experiments

Transient studies were performed in the TAP-2 reactor, which has been described in detail previously [28]. The catalyst (ca. 200 mg; $d_p = 250$–355 μm) was packed between two layers of quartz of the same particle size in the microreactor ($\varnothing_{in} \sim 6$ mm) made of quartz. Before transient experiments, the catalyst was pretreated at ambient pressure either in an O_2 flow (50 $cm^3_{STP}\,min^{-1}$) at 823 K for 2 h or in an H_2 flow (H_2/Ar = 5/95; 50 $cm^3_{STP}\,min^{-1}$) at 373 K for 30 min. The pretreated catalyst samples are denoted as preoxidized and prereduced, respectively. According to our previous characterisation studies [15], the prereduced sample contains both metallic Ag^0 and Ag_2O species, whereas nanosized Ag_2O clusters are the only species in the preoxidized sample. After the respective pretreatment, the catalyst was exposed to vacuum (ca. 10^{-5} Pa), and pulse experiments were carried out in the temperature range of 423–723 K. The following transient experiments were performed:

- To understand the effect of O_2 on NH_3–NO interactions, O_2/Xe = 1/1 and $^{15}NH_3/^{14}NO$/Ne = 1/1/1 or $^{14}NH_3/^{15}NO$/Ne = 1/1/1 mixtures were sequentially pulsed with different time delays (Δt) between the mixtures. The time delay was varied from 0 to 2 s.
- NO reduction with NH_3 in the presence of H_2 was studied by means of pulse experiments using $^{15}NH_3/^{14}NO/H_2$/Ne = 1/1/10/1 or $^{14}NH_3/^{15}NO/H_2$/Ne = 1/1/10/1 mixtures.
- Ternary $NH_3/NO/H_2/O_2$ interactions were investigated in the sequential pulse mode using O_2/Xe = 1/1 and $^{15}NH_3/^{14}NO/H_2$/Ne = 1/1/10/1 mixtures with Δt of 0 s.
- To determine whether N-containing intermediates, which may be formed and retained on the catalyst surface during the NH_3–NO–H_2 or NH_3–NO–H_2–O_2 reactions, are oxidized by oxygen, an O_2/Xe = 1/1 mixture was pulsed at 723 K over the catalyst after the above reactions were carried out at different temperatures (423–723 K).

Due to technical reasons, isotopically labeled nitric oxide (^{15}NO) was used in the experiments with the preoxidized sample, whereas isotopically labeled ammonia ($^{15}NH_3$) was used in the experiments with the prereduced sample. The following gases were applied: H_2 (5.0), Ne (4.5), Xe (4.0), O_2 (4.5), ^{14}NO (2.5), $^{14}NH_3$ (2.5), $^{15}NH_3$ (99.9% atoms of ^{15}N), and ^{15}NO (98% atoms of ^{15}N). Isotopically labeled ammonia and nitric oxide were purchased from ISOTEC. Transient responses were monitored at atomic mass units (AMUs) related to reactants, reaction products, and inert gases at the reactor outlet

using a quadruple mass spectrometer (HAL RC 301 Hiden Analytical). The following AMUs were analyzed: 132 (Xe), 46 ($^{14}NO_2$, $^{15}N^{15}NO$), 45 ($^{15}N^{14}NO$), 44 ($^{14}N^{14}NO$), 32 (O_2), 31 (^{15}NO, $H^{14}NO$), 30 ($^{14}N^{14}NO$, ^{14}NO, $^{15}N^{15}N$), 29 ($^{15}N^{14}N$), 28 ($^{14}N^{14}NO$, $^{14}N^{14}N$), 20 (Ne), 18 (H_2O, $^{15}NH_3$), 17 ($^{14}NH_3$, $^{15}NH_3$, H_2O, OH), and 2 (H_2). For each AMU, pulses were repeated 10 times and averaged to improve the signal-to-noise ratio. In the experiments on O_2 pulsing over the catalyst prepulsed by NH_3–NO–O_2 or NH_3–NO–H_2–O_2 mixtures, transient responses of O_2 and reaction products were recorded without averaging. The concentrations of feed components and reaction products were determined from the respective AMUs using standard fragmentation patterns and sensitivity factors arising from the different ionisation probabilities of individual compounds. The relative sensitivities were determined as ratios of the areas under the response signals of each compound related to the area under the response signal of inert gas. The respective areas were corrected according to the contribution of fragmentation pattern of other compounds to the measured AMU signal. The fragmentation patterns and respective sensitivities of feed components and reaction products were determined from separate calibration experiments in which a mixture of the calibrated gas and inert standard was pulsed in the reactor filled with SiO_2 particles. There is assumed to be no difference in the calibration values between the nonisotopically labeled and isotopically labeled compounds.

3. Results

Sections 3.1 and 3.2 describe the results of transient experiments of NO reduction by NH_3 in the presence and absence of O_2 and H_2 over preoxidized and prereduced $2Ag/Al_2O_3$ samples, respectively. In Section 3.2 particular attention is paid to the formation of surface intermediates during the NH_3–NO–O_2 reaction and their transformation to various gas-phase products on interaction with O_2. Finally, a detailed mechanistic concept considering the role of O_2 and H_2 in the NO–NH_3 interactions over $2Ag/Al_2O_3$ under transient vacuum conditions is suggested.

3.1. Transient experiments over preoxidized Ag/Al_2O_3

3.1.1. $^{14}NH_3$–^{15}NO–O_2 interactions

The preoxidized $2Ag/Al_2O_3$ sample was used without any further treatment. The effect of oxygen on the NO–NH_3 interaction was studied in the temperature range of 423–723 K by sequential pulsing of O_2/Xe = 1/1 and $^{14}NH_3/^{15}NO$/Ne = 1/1/1 mixtures with time delays (Δt) varying from 0 to 0.5 s between the mixtures. This procedure helps to determine whether adsorbed oxygen species (formed in the O_2 pulse) influence the product distribution in the $^{14}NH_3$–^{15}NO pulse. Conversely, it can also show whether surface intermediates that can be formed in the $^{14}NH_3$–^{15}NO pulse and retained on the catalyst surface are oxidized in the O_2 pulse.

$^{15}N_2O$, $^{14}N^{15}N$, and $^{14}N_2$, as well as a signal at an AMU of 30 (resulting from ^{14}NO or $^{15}N_2$), were detected at the reactor outlet in the $^{14}NH_3$–^{15}NO pulse. Only traces of $^{14}N^{15}N$ and the signal at an AMU of 30 (resulting from ^{14}NO or $^{15}N_2$) were detected in the O_2 pulse. This indicates that N-containing species formed during the $^{14}NH_3$–^{15}NO pulse either are not stabilized on the catalyst surface or are not significantly oxidized by O_2. The appearance of different nitrogen isotopes ($^{14}N^{15}N$ and $^{14}N_2$) in the reaction products proves activation of nitric oxide and ammonia on the catalyst surface. However, the yield of all detected reaction products was <0.5% even at 723 K; that is, the preoxidized $2Ag/Al_2O_3$ sample showed rather low activity in the NH_3-SCR under transient conditions in the temperature range 423–723 K.

3.1.2. $^{14}NH_3$–^{15}NO–O_2–H_2 interactions

To prove whether H_2 influences the NH_3–NO interactions over the preoxidized $2Ag/Al_2O_3$ catalyst, transient experiments with a $^{14}NH_3/^{15}NO/H_2$/Ne = 1/1/10/1 mixture were performed at 423 and 723 K. In addition, $^{14}NH_3/^{15}NO/H_2$/Ne = 1/1/10/1 and O_2/Xe = 1 mixtures were pulsed simultaneously at the same temperatures. In the latter experiments, the ratio of O_2 to $^{14}NH_3$ was >5. Compared with the results in Section 3.1.1, no significant changes in catalytic performance of the preoxidized $2Ag/Al_2O_3$ catalyst were observed in the presence of H_2. Thus, the accelerating effect of H_2 on the NH_3-SCR of NO as observed at ambient pressure [10] does not appear over the preoxidized $2Ag/Al_2O_3$ catalyst under transient vacuum conditions.

Another important observation is the influence of oxygen on the interaction of nitric oxide with the preoxidized $2Ag/Al_2O_3$ catalyst. Fig. 1 compares the shapes of transient responses of ^{15}NO on pulsing of the $^{14}NH_3/^{15}NO/H_2$/Ne = 1/1/10/1 mixture and simultaneous pulsing of the O_2/Xe = 1 and $^{14}NH_3/^{15}NO/H_2$/Ne = 1/1/10/1 mixtures at 423 and 723 K. This figure demonstrates that the transient response of ^{15}NO becomes broader and shifts to longer times when O_2 is present in the reaction mixture. Such changes in the shape of the transient responses indicate an increased ability of the preoxidized $2Ag/Al_2O_3$ catalyst for NO adsorption and slower NO desorption in the presence of O_2. These findings can be reconciled with earlier results of FTIR measurements [17] indicating enhanced formation of nitrate surface intermediates in the simultaneous presence of H_2 and O_2 in an NH_3–NO mixture.

Summarizing the foregoing results, the preoxidized $2Ag/Al_2O_3$ catalyst is not found to be active for the NH_3-SCR reaction in the presence and absence of O_2 under transient conditions of the TAP reactor. In addition, H_2 does not influence the NH_3-SCR reaction. Possible explanations for these phenomena are given in Section 4, taking into account the results of NH_3–NO–O_2–H_2 interactions over the prereduced $2Ag/Al_2O_3$ catalyst.

3.2. Transient experiments over prereduced Ag/Al_2O_3

3.2.1. $^{15}NH_3$–^{14}NO interactions

NH_3-SCR of NO was studied over prereduced $2Ag/Al_2O_3$ by pulsing a $^{15}NH_3$–^{14}NO mixture ($^{15}NH_3/^{14}NO$/Ne = 1/1/1) in the temperature range 423–723 K. In contrast to the results given in Section 3.1.1, the prereduced $2Ag/Al_2O_3$ catalyst

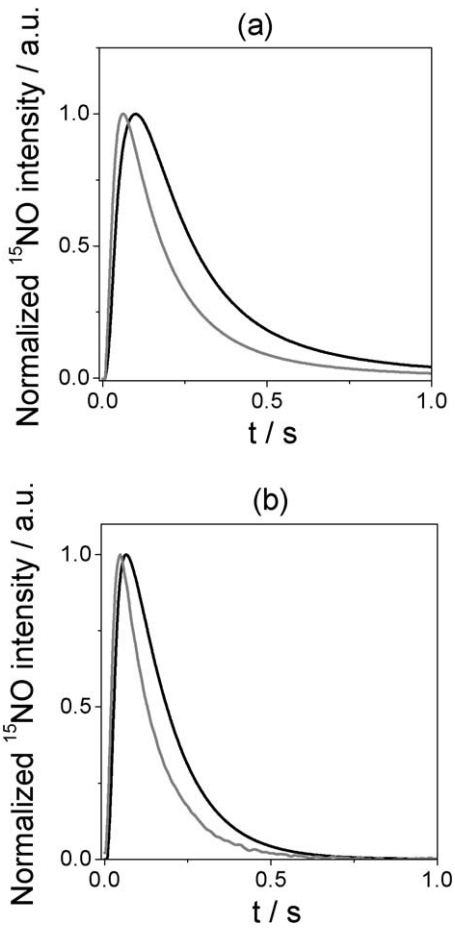

Fig. 1. Normalized transient responses of ^{15}NO after single pulsing of $^{14}NH_3/^{15}NO/H_2/Ne = 1/1/10/1$ (grey lines) as well as simultaneous pulsing of $O_2/Xe = 1$ and $^{14}NH_3/^{15}NO/H_2/Ne = 1/1/10/1$ mixtures (black lines) over preoxidized $2Ag/Al_2O_3$ at 423 (a) and 723 K (b). Pulse sizes of O_2 and ^{15}NO are ca. $6 \cdot 10^{15}$ and 10^{15} molecules, respectively.

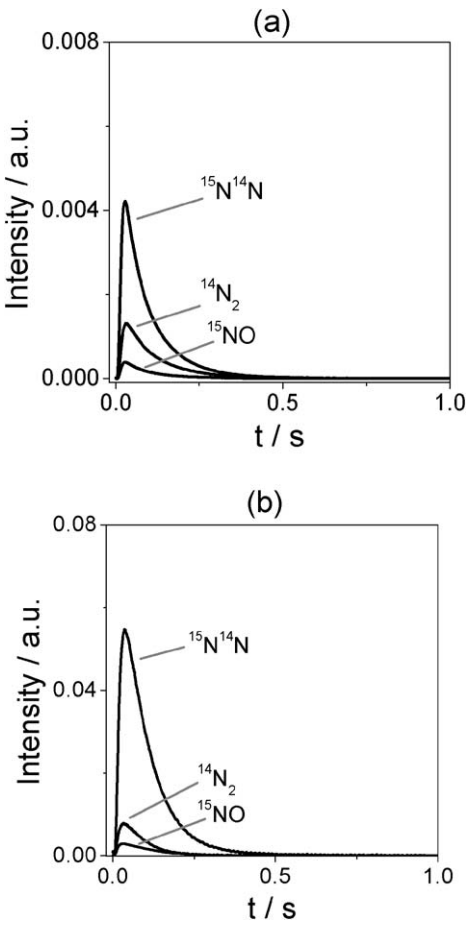

Fig. 2. Transient responses of $^{15}N^{14}N$, $^{14}N_2$ and ^{15}NO upon single pulsing of $^{15}NH_3/^{14}NO/Ne = 1/1/1$ (a) as well as simultaneous pulsing of $O_2/Xe = 1$ and $^{15}NH_3/^{14}NO/Ne = 1/1/1$ mixtures (b) over prereduced $2Ag/Al_2O_3$ at 723 K. Pulse sizes of O_2 and $^{15}NH_3$ are ca. $5 \cdot 10^{15}$ and $5 \cdot 10^{14}$ molecules, respectively.

showed considerably higher activity. $^{14}N_2$ was detected as the main N-containing product; its yield increased from ca. 3% at 423 K to 7% at 723 K. Formation of $^{14}N_2$ implies a decomposition reaction of ^{14}NO on prereduced Ag yielding ^{14}N and O atoms (Eq. (1)). The possibility that ^{14}NO is adsorbed before ^{14}NO dissociates to ^{14}N and O cannot be excluded. Two ^{14}N atoms recombine, giving $^{14}N_2$ (Eq. (2)). Nitric oxide has been also reported to dissociate over Pt-based catalysts [1,26,29,30] and Cu-modified zeolites [31,32],

$$^{14}NO_{(g)} \rightarrow {}^{14}N_{(s)} + O_{(s)} \quad (1)$$

and

$$^{14}N_{(s)} + {}^{14}N_{(s)} \rightarrow {}^{14}N_{2(g)}, \quad (2)$$

where (s) and (g) denote the fixation of species to the metal surface and gaseous components, respectively.

Identification of $^{15}N^{14}N$ in the reaction products indicates a coupling reaction between $^{15}NH_3$ and ^{14}NO. But this reaction pathway is not relevant, because only traces of $^{15}N^{14}N$ were observed. Besides $^{14}N_2$ and $^{15}N^{14}N$, various isotopically labeled nitrous oxides ($^{15}N_2O$, $^{15}N^{14}NO$, and $^{14}N_2O$) were also identified as minor reaction products. The appearance of ^{15}N-containing reaction products implies that $^{15}NH_3$ becomes dehydrogenated by oxygen species. Equation (3) suggests the first step of ammonia dehydrogenation by oxygen species. It is concluded that oxygen species participating in this reaction originate from the aforementioned decomposition of nitric oxide (Eq. (1)). The $^{15}NH_2$ fragments thus formed can be further dehydrogenated, yielding reactive ^{15}NH and ^{15}N species. At this stage, it is impossible to conclude which $^{15}NH_x$ ($x = 0$–2) fragments participate in nitrogen ($^{14}N^{15}N$) and nitrous oxide ($^{14}N^{15}NO$ and $^{15}N_2O$) formation,

$$^{15}NH_{3(s)} + O_{(s)} \rightarrow {}^{15}NH_{2(s)} + OH_{(s)}. \quad (3)$$

3.2.2. *$^{15}NH_3$–^{14}NO–O_2 interactions*

On simultaneous pulsing of $^{15}NH_3/^{14}NO/Ne = 1/1/1$ and $O_2/Xe = 1/1$ mixtures (with $O_2/^{15}NH_3$ ratio >8), $^{15}N_2O$, $^{15}N^{14}NO$, $^{14}N_2O$, ^{15}NO, $^{15}N^{14}N$, and $^{14}N_2$ were identified as reaction products. $^{15}N_2$ formed from $^{15}NH_3$ oxidation cannot be unambiguously determined in the presence of ^{14}NO (which is a feed component) by mass spectroscopic analysis, because both components have a signal at an AMU of 30. Therefore, $^{15}N_2$ formation is not discussed in this section, but is treated in Section 3.2.4.

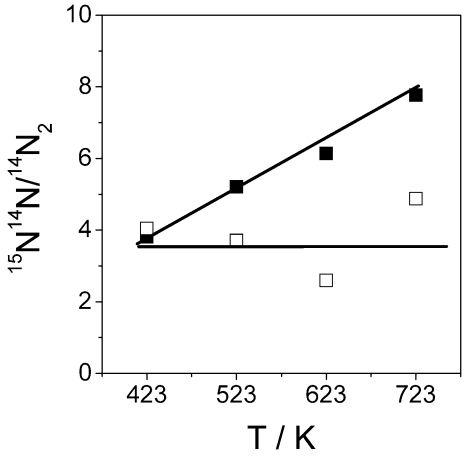

Fig. 3. Distribution of various nitrogen isotopes upon simultaneous pulsing of O_2/Xe = 1 and $^{15}NH_3/^{14}NO$/Ne = 1/1/1 mixtures (solid symbols) as well as simultaneous pulsing of O_2/Xe = 1 and $^{15}NH_3/^{14}NO/H_2$/Ne = 1/1/10/1 (open symbols) over pre-reduced $2Ag/Al_2O_3$. Pulse sizes are as in capture of Fig. 2.

Fig. 2 compares transient responses of major products ($^{15}N^{14}N$, $^{14}N_2$, and ^{15}NO) detected at the reactor outlet on pulsing of $^{15}NH_3/^{14}NO$/Ne = 1/1/1 mixture as well as on simultaneous pulsing of O_2/Xe = 1 and $^{15}NH_3/^{14}NO$/Ne = 1/1/1 mixtures at 723 K. Note in particular that the signal intensities in Fig. 2a (pulsing of $^{15}NH_3/^{14}NO$/Ne = 1/1/1 mixture) are ca. 10 times lower than those in Fig. 2b (simultaneous pulsing of O_2/Xe = 1 and $^{15}NH_3/^{14}NO$/Ne = 1/1/1 mixtures). This means that the concentration of reaction products is considerably higher in the NO–NH_3–O_2 interactions than in the NO–NH_3 interactions. In other words, the presence of oxygen strongly enhances the activity of the prereduced $2Ag/Al_2O_3$ catalyst in the SCR of NO with NH_3 under transient vacuum conditions. This conclusion closely agrees with the results of many previous studies over various catalytic systems at ambient pressure [33].

The occurrence of ^{15}NO in reaction products results from oxidation of $^{15}NH_3$. It is well known that ammonia is oxidised to nitric oxide over various oxide catalysts and noble metals including silver [34–36].

Among the identified nitrogen isotopes ($^{15}N^{14}N$ and $^{14}N_2$), $^{15}N^{14}N$ was the main isotopic trace. Fig. 3 (solid symbols) illustrates the ratio of $^{15}N^{14}N/^{14}N_2$ as a function of temperature. This ratio is ca. 4 at 423 K and increases with increasing temperature. This observation leads to the conclusion that direct ^{14}NO decomposition to $^{14}N_2$ (Eqs. (1) and (2)) is less favored at higher temperature compared with a coupling reaction between ^{14}NO and $^{15}NH_3$ yielding $^{15}N^{14}N$. Previous mechanistic concepts of NO–NH_3 interactions over a Pt/Al_2O_3 catalyst [37] and Pt-based gauzes [27] consider the formation of molecular nitrogen with mixed isotopically labeled nitrogen atoms via a complex reaction between adsorbed NO and NH_x ($x = 1$–2) fragments (Eq. (4)). It cannot be excluded that gas-phase NO reacts with adsorbed NH_x fragments. Based on this mechanistic concept, an increase in the ratio of $^{15}N^{14}N/^{14}N_2$ with temperature can be explained by temperature-accelerated oxygen activation yielding active oxygen species, which participate in ammonia dehydrogenation (Eq. (3)) to give reactive NH_x fragments, which take part in nitrogen formation (Eq. (4)),

$$^{15}NH_{x(s)} + {}^{14}NO_{(s)} \rightarrow {}^{15}N^{14}N_{(g)} + H_xO_{(s)}. \quad (4)$$

Based on the identification of three nitrous oxide isotopes ($^{15}N_2O$, $^{15}N^{14}NO$, and $^{14}N_2O$), three formal origins of their production can be suggested: (i) $^{15}N_2O$ originates from ammonia only; (ii) $^{14}N_2O$ is a product of ^{14}NO transformations; and (iii) $^{15}N^{14}NO$ is a product of a coupling reaction of $^{15}NH_3$ with ^{14}NO. The contribution of individual isotopically labeled nitrous oxides ($^{15}N_2O$, $^{15}N^{14}NO$, and $^{14}N_2O$) to the total nitrous oxide production is shown in Fig. 4a as a function of temperature. The contribution was calculated as the ratio of mole fraction of individual nitrous oxide isotope to the sum of mole fractions of all detected nitrous oxide isotopes. Fig. 4a demonstrates that $^{15}N^{14}NO$ prevails at all temperatures, but its contribution to total nitrous oxide production decreases with increasing temperature. $^{15}N_2O$, which is formally formed from two $^{15}NH_3$ molecules, is the minor product in the temperature range 423–623 K. The contribution of ^{14}NO transformation to $^{14}N_2O$ is more or less independent of temperature and similar to that of $^{15}N_2O$ at 723 K.

3.2.3. $^{15}NH_3$–^{14}NO–O_2–H_2 interactions

To determine whether the NH_3-SCR reaction in the presence of O_2 is influenced by hydrogen, $^{15}NH_3/^{14}NO/H_2$/Ne = 1/1/10/1 and O_2/Xe = 1 mixtures were pulsed simultaneously over prereduced $2Ag/Al_2O_3$ in the temperature range of 432–723 K. The $O_2/^{15}NH_3$ ratio was >7. As in the case of $^{15}NH_3$–^{14}NO–O_2 interactions, $^{15}N_2O$, $^{15}N^{14}NO$, $^{14}N_2O$, ^{15}NO, $^{15}N^{14}N$, and $^{14}N_2$ were the main N-containing reaction products detected at the reactor outlet. Hydrogen was not found to significantly influence the activity of the prereduced $2Ag/Al_2O_3$ catalyst in the NH_3-SCR reaction; however, the product distribution was influenced by the presence of hydrogen. Fig. 3 compares the ratio of $^{15}N^{14}N/^{14}N_2$ in the $^{15}NH_3$–^{14}NO–O_2 and $^{15}NH_3$–^{14}NO–O_2–H_2 interactions at different temperatures. $^{15}N^{14}N$ is the main nitrogen isotope in the presence and absence of hydrogen; however, in contrast to the $^{15}NH_3$–^{14}NO–O_2 interactions, where the ratio of $^{15}N^{14}N/^{14}N_2$ increases with rising temperature, this ratio does not depend on temperature in the presence of H_2. This observation can be explained in the following way. From previous studies of H_2 activation on Ag/Al_2O_3 [38] and even on Ag/SiO_2 catalysts [39], it is known that molecular hydrogen dissociates over metallic silver, yielding adsorbed hydrogen species. These hydrogen species may promote direct NO decomposition to N_2, as suggested earlier for Pt-based gauzes [27]. Thus, the formation of both $^{14}N_2$ and $^{15}N^{14}N$ is enhanced by temperature to a comparable extent, and the ratio of $^{15}N^{14}N/^{14}N_2$ remains constant. In the absence of hydrogen, this promotion of NO dissociation plays no role; therefore, $^{15}N^{14}N$ formation, in contrast to $^{14}N_2$ production, increases with increasing temperature due to increased ammonia dehydrogenation by oxygen species formed via O_2 activation.

Figs. 4a and 4b compare the contribution of individual nitrous oxide isotopes ($^{15}N_2O$, $^{15}N^{14}NO$, $^{14}N_2O$) to the total

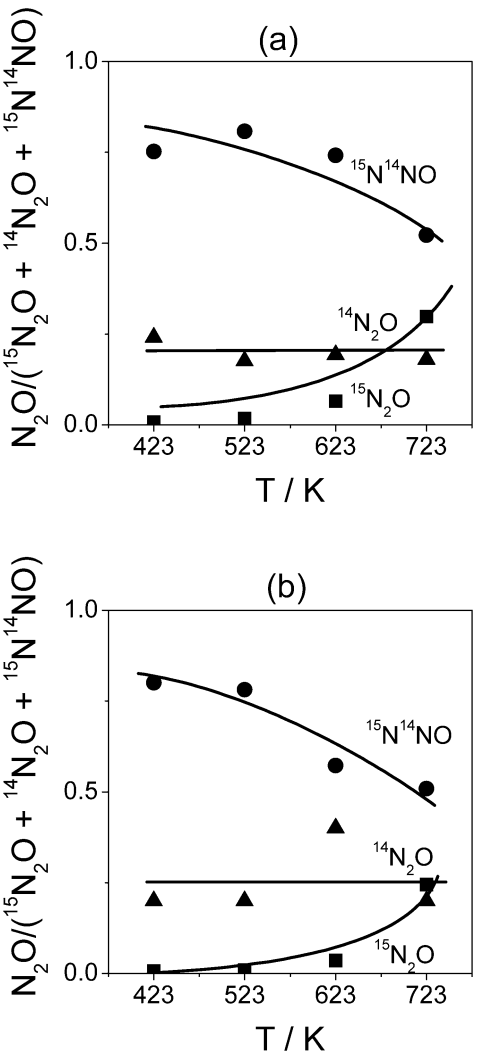

Fig. 4. Distribution of various nitrous oxide isotopes during simultaneous pulsing of O_2/Xe = 1 and $^{15}NH_3/^{14}NO$/Ne = 1/1/1 mixtures (a) as well as simultaneous pulsing of O_2/Xe = 1 and $^{15}NH_3/^{14}NO/H_2$/Ne = 1/1/10/1 (b) over prereduced $2Ag/Al_2O_3$. Pulse sizes are as in capture of Fig. 2.

nitrous oxide production in the $^{15}NH_3$–^{14}NO–O_2 and $^{15}NH_3$–^{14}NO–O_2–H_2 interactions, respectively. It is obvious that hydrogen does not influence the distribution of isotopic labeled nitrous oxides; $^{15}N^{14}NO$ is the main isotope at all temperatures. $^{15}NH_3$ oxidation to $^{15}N_2O$ plays a significant role only at 723 K. Another interesting observation is the influence of hydrogen on the overall N_2O selectivity, as depicted in Fig. 5. This figure reveals a strong decrease in N_2O selectivity in the presence of hydrogen, corresponding to experimental findings under steady-state ambient pressure conditions [10].

3.2.4. Reaction of surface intermediates with oxygen

The existence and reactivity of strongly adsorbed surface intermediates formed during the NH_3-SCR of NO in the presence of O_2 was proven in the following manner. An $^{15}NH_3$–^{14}NO–O_2 mixture was pulsed over the prereduced $2Ag/Al_2O_3$ catalyst at a specific reaction temperature (423–723 K), followed by O_2 pulsing (ca. 4 μmol of O_2) at 723 K. $^{15}N_2O$, $^{15}N^{14}NO$,

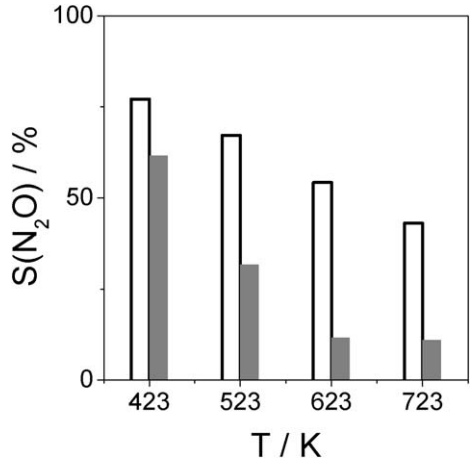

Fig. 5. Total N_2O selectivity as a function of temperature upon simultaneous pulsing of O_2/Xe = 1 and $^{15}NH_3/^{14}NO$/Ne = 1/1/1 mixtures (empty bars) as well as simultaneous pulsing of O_2/Xe = 1 and $^{15}NH_3/^{14}NO/H_2$/Ne = 1/1/10/1 (grey bars) over prereduced $2Ag/Al_2O_3$. Pulse sizes are as in capture of Fig. 2.

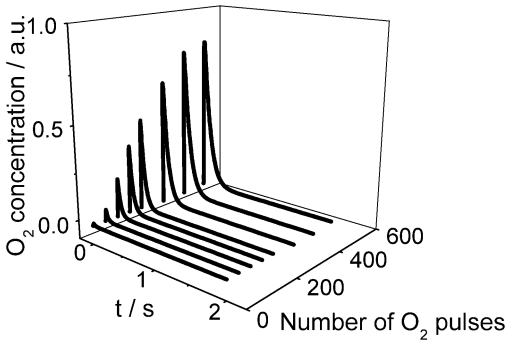

Fig. 6. O_2 concentration measured at the reactor outlet upon O_2 pulsing at 723 K over $2Ag/Al_2O_3$ having been prepulsed by $^{15}NH_3$–^{14}NO–O_2 at 723 K. O_2 pulse size is $5 \cdot 10^{15}$ molecules.

$^{14}N_2O$, $^{15}N^{14}N$, $^{14}N_2$, ^{15}NO, and a signal at an AMU of 30 were identified in the O_2 pulses. All nitrous oxide isotopes were minor products; $^{15}N^{14}N$ and the signal at an AMU of 30 were detected as major products. The appearance of various reaction products after O_2 pulsing over the catalyst that was prepulsed by $^{15}NH_3$–^{14}NO–O_2 proves the presence of surface ^{14}N- and ^{15}N-containing intermediates that react with O_2, yielding gas-phase products. These surface intermediates were formed during NH_3-SCR and remained on the catalyst surface even at 723 K.

A typical profile of the reactor outlet concentration of oxygen as a function of the number of oxygen pulses is given in Fig. 6. Clearly, O_2 concentration is very low in the first O_2 pulses but increases with the amount of O_2 pulsed. Contrary to the profile of O_2 concentration in Fig. 6, the outlet concentration of all detected reaction products is highest in the first O_2 pulse and decreases with an increasing number of O_2 pulses. Fig. 7 shows concentration profiles of $^{15}N^{14}N$, $^{14}N_2$, ^{15}NO, and the signal at an AMU of 30. Similar profiles were also observed for other products. Such concentration profiles of O_2 and reaction products can be explained as follows. The concentration of surface nitrogen-containing species is highest after the $^{15}NH_3$–

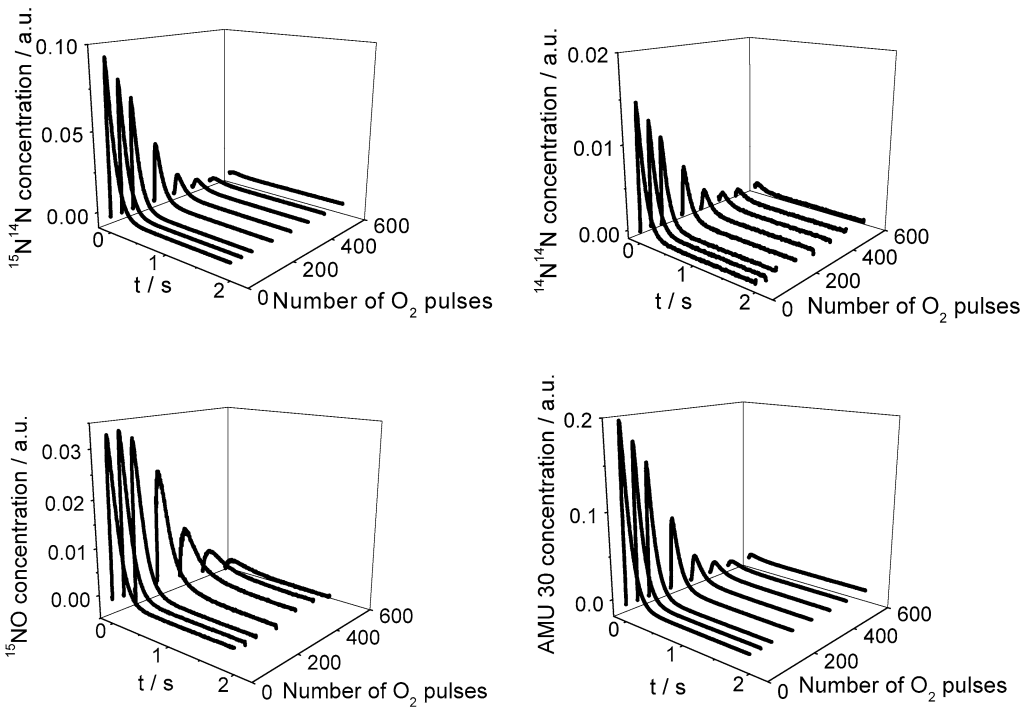

Fig. 7. $^{15}N^{14}N$, $^{14}N_2$, ^{15}NO and signal at an AMU of 30 measured at the reactor outlet upon O_2 pulsing at 723 K over $2Ag/Al_2O_3$ having been prepulsed by $^{15}NH_3$–^{14}NO–O_2 at 723 K. O_2 pulse size is $5 \cdot 10^{15}$ molecules.

^{14}NO–O_2 pulse experiments; therefore, oxygen consumption is expected to be high in the early O_2 pulses due to the reaction with adsorbed nitrogen-containing species. With an increasing number of O_2 pulses, the degree of O_2 consumption should decrease, because nitrogen-containing species are consumed. Accordingly, the concentration of gas-phase reaction products should be highest in the first O_2 pulses and decrease with an increasing number of pulses.

We now consider the nature of signal at an AMU of 30. Based on mass spectroscopic analysis, this signal can be ascribed to either ^{14}NO or $^{15}N_2$. The appearance of ^{14}NO and $^{15}N_2$ on O_2 pulsing may be due to O_2-assisted ^{14}NO desorption or to oxidative transformation of ^{15}N-containing species, respectively. The latter species can be transformed not only to $^{15}N_2$, but also to $^{15}N^{14}N$ and ^{15}NO, which were experimentally identified as well (see Fig. 7). Because transient responses of any detected gas-phase products contain information on all processes occurring in the TAP reactor during a pulse experiment, detailed analysis of the shape and appearance order of $^{15}N^{14}N$, ^{15}NO, and the signal at AMU 30 may indicate whether the signal at AMU 30 belongs to ^{14}NO or to $^{15}N_2$.

Fig. 8 compares normalized and averaged transient responses of $^{15}N^{14}N$, ^{15}NO, and the signal at AMU 30 detected on O_2 pulsing at 723 K over $2Ag/Al_2O_3$ that was prepulsed by $^{15}NH_3$–^{14}NO–O_2 at 723 K. This figure clearly shows that the normalized transient response of ^{15}NO is broader and shifted to a longer time compared with those of $^{15}N^{14}N$ and the signal at AMU 30, which are very similar to one another. In addition, the normalized transient response of ^{15}NO has a long tail, similar to that of ^{14}NO observed on pulsing $^{15}NH_3$–^{14}NO–O_2 (Fig. 1b). Because the normalized transient response of the signal at AMU 30 does not have a long tail and is very similar to that of $^{15}N^{14}N$, the signal at AMU 30 may belong mainly to $^{15}N_2$.

Summarizing the results of this section, nitrogen-containing species originating from both ^{14}NO and $^{15}NH_3$ are formed and retained on the surface of prereduced $2Ag/Al_2O_3$ catalyst during ^{14}NO reduction by $^{15}NH_3$. These species are oxidized by O_2, yielding nitrogen, nitric, and nitrous oxides, with the latter being the minor products. Based on the distribution of nitrogen isotopes, nitrogen-containing species originating from $^{15}NH_3$ are the main surface fragments.

4. Discussion

4.1. Mechanistic aspects of the NH_3-SCR reaction in the absence and presence of O_2

The results presented in Section 3.1.1 clearly demonstrate very low activity of preoxidized $2Ag/Al_2O_3$ catalyst in the NH_3-SCR reaction both without and with oxygen under transient vacuum conditions in the temperature range of 423–723 K. Indeed, consumption of NO and NH_3 was observed, but no adequate product formation was detected. This means that adsorption (including, presumably, the alumina surface) occurs, but reaction on the oxidized catalyst surface is negligible. This finding agrees well with results previously reported by Richter et al. [10] on the NH_3-SCR reaction over Ag/Al_2O_3 catalysts (1 and 5 wt% Ag loading) under ambient pressure conditions (1000 ppm NO, 1000 ppm NH_3, 6% O_2, 7% H_2O).

The low activity of the oxidized $2Ag/Al_2O_3$ catalyst can be explained as follows. Taking into account numerous mecha-

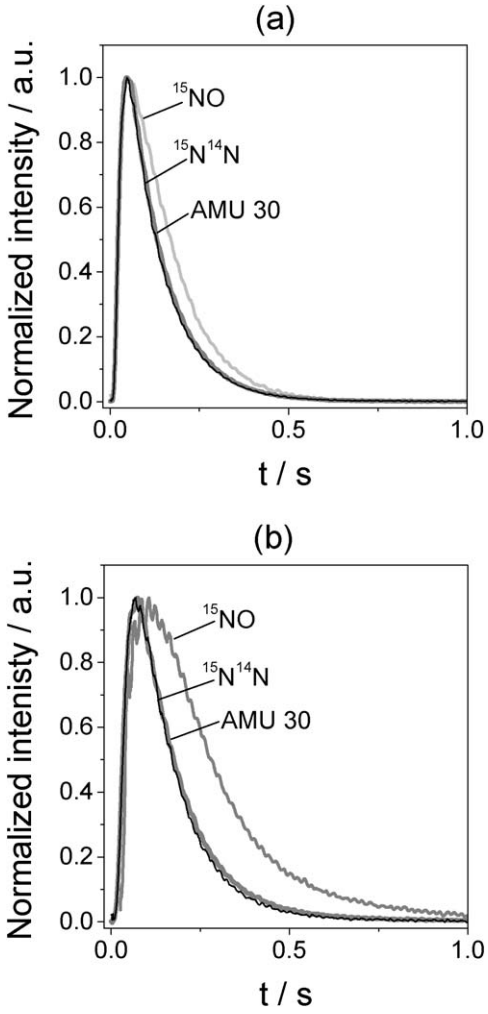

Fig. 8. Normalized transient responses of $^{15}N^{14}N$, ^{15}NO and signal at AMU of 30 measured at the reactor outlet upon O_2 pulsing at 723 K over $2Ag/Al_2O_3$ having been prepulsed by $^{15}NH_3$–^{14}NO–O_2 at 723 K.

nistic studies on the NH_3-SCR reaction over various catalytic systems [27,33,37,40], and including the results in Section 3.2.2, NH_x fragments play a significant role in the reaction. In addition to direct NO decomposition (Eq. (1)), they also open a new reaction pathway for NO decomposition: NH_3-assisted NO decomposition (Eq. (4)). Such NH_x fragments are formed via reaction of ammonia with surface oxygen species (Eq. (3)). Surface oxygen species are represented either by lattice oxygen in the case of oxide catalytic materials or by adsorbed oxygen species originating from either O_2 adsorption or NO decomposition (Eq. (1)) in the case of metal-based catalysts. Oxygen adsorption occurs on oxide and metallic sites. In contrast to oxygen adsorption, NO decomposition (Eq. (1)) occurs preferentially on reduced sites [1,26,29–32]. Based on the foregoing discussion, low activity of the preoxidized $2Ag/Al_2O_3$ catalyst in the NH_3-SCR reaction without and with O_2 is related to its low capability for ammonia activation. Oxygen species stabilized in the preoxidized $2Ag/Al_2O_3$ catalyst are not assumed to be active for hydrogen abstraction from NH_3 molecules. According to a previous transient study of methanol oxidation over polycrystalline Ag [41], oxidized Ag species do not favour O_2 adsorption. Moreover, the preoxidized $2Ag/Al_2O_3$ catalyst is not active for NO decomposition (Eq. (1)), which is a source of reactive oxygen species.

The results presented in Sections 3.2.1 and 3.2.2 support the foregoing discussion. Prereduced $2Ag/Al_2O_3$ catalyst showed considerably higher activity for the ^{14}NO-SCR reaction with $^{15}NH_3$ without O_2 compared with the preoxidized one. This is due to an increased activity of prereduced Ag species for ^{14}NO decomposition, as proven by identification of $^{14}N_2$ as the main nitrogen isotope (Section 3.2.2). $^{15}N^{14}N$ was also observed, but in lower amounts. The formation of $^{15}N^{14}N$ implies $^{15}NH_3$ dehydrogenation by reactive oxygen species (Eq. (4)) originating from ^{14}NO decomposition (Eq. (1)). If O_2 is present in a $^{15}NH_3$–^{14}NO mixture, then the catalytic conversion increases considerably with nitrogen formation involving nitrogen atoms both from ^{14}NO and $^{15}NH_3$ (Eq. (4)). In contrast to the SCR reaction of ^{14}NO with $^{15}NH_3$ in the absence of O_2, $^{15}N^{14}N$ becomes the main nitrogen isotope in the presence of O_2 (Fig. 3). This means that NH_3-assisted NO decomposition (Eq. (4)) is the main reaction pathway of nitrogen production in the NH_3-SCR reaction. The accelerating effect of oxygen is related to the activation of gas-phase O_2 over reduced Ag species, yielding reactive oxygen species. Resulting oxygen species dehydrogenate ammonia and enable efficient liberation of molecular nitrogen, with one N coming from NH_3 and one N coming from NO. Even if the same surface intermediates were formed on the preoxidized catalyst, the further conversion of these intermediates would not be feasible, because of the missing active oxygen. Concerning the nature of active oxygen species, it is well established that O_2 adsorption over silver at different temperatures results in stabilization of various adsorbed molecular and atomic oxygen species [42–44]. Molecular and atomic oxygen species are formed at low and medium temperatures (up to 473 K), whereas subsurface and bulk-dissolved oxygen species are formed at higher temperatures. Due to the variety of oxygen species on silver, it is not possible at this stage to precisely identify the nature of oxygen species responsible for the dehydrogenation of ammonia.

Another possible role of oxygen in catalyzing the NH_3-SCR reaction can be understood taking into account the results presented in Section 3.2.4. As shown in Fig. 7, $^{15}N_2O$, $^{15}N^{14}NO$, $^{14}N_2O$, ^{15}NO, $^{15}N_2$, $^{15}N^{14}N$, and $^{14}N_2$ are formed on pulsing of O_2 on $2Ag/Al_2O_3$ directly after performing the NH_3-SCR reaction with O_2. Compared with other reaction products, $^{15}N_2$ and $^{15}N^{14}N$ were identified in significant amounts, with the former being the major product. This means that $^{15}NH_x$ or $^{15}NH_x$–^{14}NO ($x = 0$–2) intermediates are formed during the NH_3-SCR reaction with O_2 and retained on the surface of $2Ag/Al_2O_3$. These intermediates are oxidized by O_2, yielding various reaction products. Therefore, active oxygen species not only accelerate generation of NH_x fragments via NH_3 dehydrogenation, but also catalyze further oxidation of surface NH_x or NH_x–NO intermediates. This results in regeneration of reduced Ag sites.

4.2. H_2 effect on the NH_3-SCR reaction: comparison of steady-state ambient pressure and transient vacuum performance

In a previous study [10], cofeeding of H_2 to the NH_3-SCR of NO_x (1000 ppm NO, 1000 ppm NH_3, 6% O_2, 7% H_2O, and 0.25–1.0% H_2) resulted in a remarkable increase in the degree of NO conversion, from 10 to 100% at 323–473 K over Ag/Al_2O_3 catalysts (1 and 5 wt% Ag loading) under steady-state ambient pressure conditions. At a first glance, the present transient results do not support this finding. No clear and distinct accelerating effect of H_2 on the NH_3-SCR reaction was found over either the preoxidized (Section 3.1.2) or the prereduced (Section 3.2.3) $2Ag/Al_2O_3$ catalyst. The only exception is related to the influence of hydrogen on N_2O selectivity over the prereduced $2Ag/Al_2O_3$ catalyst. Fig. 5 clearly demonstrates that the N_2O selectivity decreases significantly in the presence of H_2. This observation corresponds to previously reported results [10], where the N_2O selectivity had a maximum of about 20% at 473–673 K for H_2-free NH_3-SCR reaction but was negligibly low with a hydrogen admixture. The observed decrease in N_2O selectivity is probably related to a decreased concentration of adsorbed oxygen species in the presence of H_2. A recent study on mechanistic aspects of nitrous oxide formation over a Pt–Rh gauze catalyst at 1073 K [45] concluded that adsorbed oxygen species are crucial to nitrous oxide formation in NO–NH_3 interactions. Moreover, the possibility that H_2 actually does not inhibit N_2O production, but rather increases its decomposition, cannot be excluded. Burch et al. [46] studied the influence of H_2 on N_2O decomposition over a Pt/SiO_2 catalyst in the temperature range of 473–773 K and explained the boosting effect of H_2 on N_2O decomposition by (i) an H-assisted N_2O dissociation mechanism and (ii) the removal of "hot" oxygen species formed from N_2O through adsorbed hydrogen species, thus regenerating active sites for N_2O decomposition.

The promoting effect of H_2 has been reported not only for SCR reaction of NO with NH_3 [10], but also with various hydrocarbons [8,9,12,15,19,46]. However, the mechanistic concept has not been clearly evaluated and is still being debated. Richter et al. [10] ascribed the accelerating effect of H_2 to reduction of nanosized Ag_2O clusters to Ag^0, which promotes NO_x dissociation. Using UV/vis [47,48] and ex situ EXAFS [49] measurements, Satokawa et al. suggested that $Ag_n^{\delta+}$ clusters are formed from isolated Ag^+ species during the SCR reaction in the presence of H_2 and are responsible for the high activity of Ag/γ-Al_2O_3 and Ag/MFI catalysts. However, Breen et al. [50] questioned the H_2-induced formation of Ag clusters based on the findings of their in situ EXAFS study. These authors found that the catalyst structure remained the same for all SCR conditions used, with or without coreductant (H_2 or CO); significant changes were observed only under reducing conditions. They concluded that the H_2 effect occurs due to a chemical interference, not due to a change in the structure of the active sites. Sazama et al. [12] proposed that the enhancing effect of hydrogen is not due to Ag cluster formation, but instead, hydrogen reacts directly either to promote the formation and storage of a reactive species that can then readily reduce NO_x or, alternatively, to remove a species acting as a poison to the SCR reaction at low temperatures. Hydrogen dissociation might occur during SCR of NO_x over Ag/Al_2O_3. It is assumed that silver hydride forms and immediately reacts with oxygen to form hydroperoxy radicals (HO_2), according to Eq. (5). Hydroperoxy radicals, which are highly active oxidants, should eventually react with NO, yielding NO_2 and hydroxyl radicals (Eq. (6)). Both of these radicals can react with hydrocarbons to their oxo/nitro derivates. To support their assumption these authors refer to the experimental observation of Burch et al. [13], who found that Ag/Al_2O_3 responds immediately (and completely reversibly) to hydrogen addition and removal with increased and decreased NO conversion, respectively:

$$Ag\text{–}H_{(s)} + O_{2(g)} \rightarrow HO'_{2(g)} + Ag^0_{(s)} \quad (5)$$

and

$$HO'_{2(g)} + NO_{(g)} \rightarrow NO_{2(g)} + OH'_{(g)}. \quad (6)$$

The time scale for changes in the number of small charged $Ag_n^{\delta+}$ clusters was estimated to be much slower, but there are no reliable figures proving this hypothesis.

The present transient study, performed under conditions in which gas-phase (radical) reactions are suppressed, does not indicate a role of radicals in the mechanism. The most important result of the present study is the identification of significant differences between preoxidized (Section 3.1) and prereduced (Section 3.2) $2Ag/Al_2O_3$ catalysts in their activity in the NH_3-SCR reaction, with the latter catalyst having the highest activity. This finding indicates that the ex situ reductive pretreatment of the $2Ag/Al_2O_3$ catalyst has transformed a marginally active sample to a highly active sample. This seems to be the crucial link between the present transient vacuum experiments and previous steady-state ambient pressure measurements [10].

Taking into account the experimental peculiarities of the TAP reactor, the finding of no direct identification of the boosting effect of H_2 on the NH_3-SCR reaction over preoxidized and prereduced $2Ag/Al_2O_3$ catalysts can be explained as follows. In contrast to the ambient pressure studies, oxidized Ag species formed during O_2 pretreatment at 873 K (see Section 2.2) cannot be sufficiently reduced with H_2 under the transient vacuum conditions, because of the small pulse size. One pulse contains ca. 10^{15} molecules of H_2, which is equivalent to 10^{-9} mol. Based on the H_2 concentration in the pulse, the number of H_2 pulses needed for a full reduction of Ag_2O to Ag^0 in the sample can be roughly estimated as ca. 10,000. Therefore, the accelerating H_2 effect would be hardly visible under the present transient conditions after a NH_3–NO–O_2–H_2 mixture was pulsed over the preoxidized $2Ag/Al_2O_3$ catalyst. If prereduced ex situ, the catalyst should already contain reduced Ag species, which remain active (nonoxidized) even on pulsing an NH_3–NO–O_2 mixture. Now, in turn, the amount of pulsed O_2 is too small to cause appreciable reoxidation of reduced silver species under transient vacuum conditions. Moreover, oxygen is consumed for NH_3 dehydrogenation. In a previous in situ UV–vis spectroscopic study [51] at ambient pressure, a reversible conversion between oxidized and reduced Ag species was established on switching from a H_2-containing mixture to an O_2-containing

mixture. This reduction process proceeds rapidly under ambient pressure flow conditions and is responsible for the boosting effect of H_2 on the NH_3-SCR, as previously suggested by Richter et al. [10].

Thus, the presence of reduced Ag species is a key factor in the accelerating effect of H_2 in the selective catalytic reduction of NO with NH_3 over a $2Ag/Al_2O_3$ catalyst. These Ag species are generated in situ during the SCR reaction in the presence of H_2 at ambient pressure. In addition, they can be created by ex situ prereduction of the oxidized sample with a diluted hydrogen flow under mild conditions (373 K). Reduced Ag species are active sites for generation of reactive oxygen species from O_2 and NO, which participate in ammonia dehydrogenation, yielding reactive NH_x fragments. The latter accelerate NO conversion to N_2.

5. Summary

A detailed mechanistic analysis of the influence of O_2 and H_2 on low-temperature (423–723 K) NH_3-SCR of NO over preoxidized and prereduced $2Ag/Al_2O_3$ catalysts was performed using transient measurements in the TAP reactor in combination with isotopically labeled ^{15}NO and $^{15}NH_3$. This led to an advanced understanding of individual reaction pathways, including surface processes. The main conclusions can be summarized as follows:

- The preoxidized $2Ag/Al_2O_3$ catalyst is not active for the reaction of NH_3–NO or NH_3–NO–O_2. This inactivity is related to the low ability of oxidized Ag species for NO decomposition and activated O_2 adsorption. Both processes generate reactive oxygen species, which participate in NH_3 dehydrogenation, yielding surface NH_x ($x = 0$–2) fragments. These ammonia intermediates are key components in the NH_3-assisted NO conversion to N_2.
- The $2Ag/Al_2O_3$ catalyst prereduced by H_2 shows considerably higher activity in the NH_3–NO reaction than the preoxidized catalyst in the absence of O_2. This high activity is due to NO dissociation to adsorbed N and O species, with the latter participating in NH_3 dehydrogenation. Based on the isotopic distribution in the ^{14}NO–$^{15}NH_3$ reaction, direct NO decomposition to N_2 is the main source of total N_2 production.
- The presence of O_2 significantly increases the activity of prereduced $2Ag/Al_2O_3$ in the NH_3-SCR reaction. Moreover, a coupling reaction between NO and NH_3 becomes the main reaction route of N_2 production, as concluded from the isotopic analysis. The increased activity and N_2 production via this coupling reaction are related to an increased generation of reactive oxygen species from O_2 over reduced Ag species. These oxygen species dehydrogenate NH_3, yielding NH_x fragments, which are important for the N_2 production via NO and NH_3 coupling. In addition, O_2 was found to regenerate active catalytic sites via decomposition of surface NH_x and NO intermediates formed during the NH_3-SCR reaction.
- It is concluded that reduction of silver surface sites is a necessary requirement for the accelerating effect of H_2 on the NH_3-SCR reaction. This conclusion is also supported by the effect of H_2 on N_2O selectivity, which decreased when hydrogen is added to the feed, independently of whether the measurements have been carried out at ambient pressure or under vacuum conditions. Under steady-state conditions, the catalyst reduction proceeds very rapidly due to the high concentration of hydrogen in the feed. In contrast, however, under transient vacuum conditions, the H_2 concentration in one pulse (ca. 10^{-8} mol) is too low to enable appropriate reduction of Ag_2O clusters. Consequently, the catalyst seemed to be only marginally active. The activity is significantly enhanced after ex situ prereduction. In this case, reduced active Ag species were generated and kept under TAP conditions.

Acknowledgments

Financial support by the federal state of Berlin (Department for Science, Research and Culture) and the EU (European Fund for Regional Development, project EFRD 2000–2005 1/0) is gratefully acknowledged.

References

[1] R. Burch, J.P. Breen, F.C. Meunier, Appl. Catal. B 39 (2002) 283.
[2] R. Burch, Catal. Rev. 46 (2004) 271.
[3] M. Koebel, M. Elsener, M. Kleemann, Catal. Today 59 (2000) 335.
[4] H.L. Fang, H.F.M. DaCosta, Appl. Catal. B 46 (2003) 17.
[5] P.L.T. Gabrielsson, Top. Catal. 28 (2004) 177.
[6] M. Koebel, M. Elsener, O. Krocher, C. Schär, R. Röthlisberger, F. Jaussi, M. Mangold, Top. Catal. 30–31 (2004) 43.
[7] W. Held, A. Koenig, T. Richter, L. Puppe, SAE Paper 900496 (1990).
[8] S. Satokawa, Chem. Lett. (2000) 294.
[9] S. Satokawa, J. Shibata, K. Shimizu, A. Satsuma, T. Hattori, Appl. Catal. B 42 (2003) 179.
[10] M. Richter, R. Fricke, R. Eckelt, Catal. Lett. 94 (2004) 115.
[11] A. Satsuma, K. Shimizu, Prog. Energy Combust. Sci. 29 (2003) 71.
[12] P. Sazama, L. Capek, H. Drobná, Z. Sobalík, J. Dedecek, K. Arveb, B. Wichterlová, J. Catal. 232 (2005) 302.
[13] R. Burch, J.P. Breen, C.J. Hill, B. Krutzsch, B. Konrad, E. Jobson, L. Cider, K. Eränen, F. Klingstedt, L.-E. Lindfors, Top. Catal. 30–31 (2004) 19.
[14] J. Shibata, K. Shimizu, S. Satokawa, A. Satsuma, T. Hattori, Phys. Chem. Chem. Phys. 5 (2003) 2154.
[15] M. Richter, U. Bentrup, R. Eckelt, M. Schneider, M.-M. Pohl, R. Fricke, Appl. Catal. B 51 (2004) 261.
[16] R. Brosius, K. Arve, M.H. Groothaert, J.A. Martens, J. Catal. 231 (2005) 344.
[17] U. Bentrup, M. Richter, R. Fricke, Appl. Catal. B 55 (2005) 213.
[18] K. Eränen, L.-E. Lindfors, F. Klingstedt, D.Y. Murzin, J. Catal. 219 (2003) 25.
[19] K. Eränen, F. Klingstedt, K. Arve, L.-E. Lindfors, D.Y. Murzin, J. Catal. 227 (2004) 328.
[20] K. Arve, E.A. Popov, F. Klingstedt, K. Eränen, L.-E. Lindfors, J. Eloranta, D.Y. Murzin, Catal. Today 100 (2005) 229.
[21] G.P. Ansell, A.F. Diwell, S.E. Golunski, J.W. Hayes, R.R. Rajaram, T.J. Truex, A.P. Walker, Appl. Catal. B 2 (1993) 81.
[22] R. Burch, P.J. Millington, A.P. Walker, Appl. Catal. B 4 (1994) 65.
[23] T. Gerlach, M. Baerns, Chem. Eng. Sci. 54 (1999) 4379.

[24] P. Denton, A. Giroir-Fendler, Y. Schuurman, H. Praliaud, C. Mirodatos, M. Primet, Appl. Catal. A 220 (2001) 141.
[25] A.R. Vaccaro, G. Mul, J. Perez-Ramirez, J.A. Moulijn, Appl. Catal. B 46 (2003) 687.
[26] J. Pérez-Ramírez, E.V. Kondratenko, V.A. Kondratenko, M. Baerns, J. Catal. 227 (2004) 90.
[27] J. Pérez-Ramírez, E.V. Kondratenko, V.A. Kondratenko, M. Baerns, J. Catal. 229 (2005) 303.
[28] J.T. Gleaves, G.S. Yablonsky, P. Phanawadee, Y. Schuurman, Appl. Catal. A 160 (1997) 55.
[29] R.J. Gorte, L.D. Schmidt, J.L. Gland, Surf. Sci. 109 (1981) 367.
[30] J.M. Bradley, A. Hopkinson, D.A. King, J. Phys. Chem. 99 (1995) 17032.
[31] M. Iwamoto, S. Yoko, K. Sakai, S. Kagawa, J. Chem. Soc., Faraday Trans. 77 (1981) 1629.
[32] M.V. Konduru, S.S.C. Chuang, J. Catal. 187 (1999) 436.
[33] V.I. Parvulescu, P. Grange, B. Delmon, Catal. Today 46 (1998) 233.
[34] V.A. Sadykov, L.A. Isupova, I.A. Zolotarskii, L.N. Bobrova, A.S. Noskov, V.N. Parmon, E.A. Brushtein, T.V. Telyatnikova, V.I. Chernyshev, V.V. Lunin, Appl. Catal. A 204 (2000) 59.
[35] L. Gang, B.G. Anderson, J. van Grondelle, R.A. van Santen, Appl. Catal. B 40 (2003) 101.
[36] M. Yang, C. Wu, C. Zhang, H. He, Catal. Today 90 (2004) 263.
[37] K. Otto, M. Shelef, J.T. Kummer, J. Phys. Chem. 74 (1970) 2690.
[38] H. Backman, J. Jensen, F. Klingstedt, J. Warna, T. Salmi, D.Y. Murzin, Appl. Catal. A 273 (2004) 303.
[39] M. Bron, E.V. Kondratenko, A. Trunschke, P. Claus, Z. Phys. Chem. 218 (2004) 405.
[40] J. Eng, C.H. Bartholomew, J. Catal. 171 (1997) 14.
[41] A.C. van Veen, O. Hinrichsen, M. Muhler, J. Catal. 210 (2004) 53.
[42] C.T. Campbell, Surf. Sci. 157 (1985) 43.
[43] X. Bao, M. Muhler, T. Schedel-Niedrig, R. Schlögl, Phys. Rev. B: Condens. Matter 54 (1996) 2249.
[44] A. Nagy, G. Mestl, T. Ruhle, G. Weinberg, R. Schlögl, J. Catal. 179 (1998) 548.
[45] E.V. Kondratenko, J. Pérez-Ramírez, Appl. Catal. A 289 (2005) 97.
[46] R. Burch, S.T. Daniells, J.P. Breen, P. Hu, Catal. Lett. 94 (2004) 103.
[47] J. Shibata, Y. Takada, A. Shichi, S. Satokawa, A. Satsuma, T. Hattori, Appl. Catal. B 54 (2004) 137.
[48] J. Shibata, Y. Takada, A. Shichi, S. Satokawa, A. Satsuma, T. Hattori, J. Catal. 222 (2004) 368.
[49] J. Shibata, K.-i. Shimizu, Y. Takada, A. Shichi, H. Yoshida, S. Satokawa, A. Satsuma, T. Hattori, J. Catal. 227 (2004) 367.
[50] J.P. Breen, R. Burch, C. Hardacre, C.J. Hill, J. Phys. Chem. B 109 (2005) 4805.
[51] M. Richter, A. Abramova, U. Bentrup, R. Fricke, J. Appl. Spectrosc. 71 (2004) 400.